Interrogating adhesion using fiber Bragg grating sensing technology

Roger D. Rasberry*[a], Garth D. Rohr[a], William K. Miller[a], Eric Udd[b], Noah T. Blach[c], Ryan A. Davis[a], Walter R. Olson[a], David Calkins[a], Allen R. Roach[a], David S. Walsh[a], James R. McElhanon[a]
[a]Sandia National Laboratories, P. O. Box 5800, MS 0888, Albuquerque, NM, USA 87185-0888
[b]Columbia Gorge Research, LLC, P. O. Box 382, 2555 NE 205th Ave, Fairview, OR USA 97024
[c]United States Air Force Academy, 2355 Fairchild Dr, Suite 2N225, US Air Force Academy, CO USA 80840-6230

ABSTRACT

The assurance of the integrity of adhesive bonding at substrate interfaces is paramount to the longevity and sustainability of encapsulated components. Unfortunately, it is often difficult to non-destructively evaluate these materials to determine the adequacy of bonding after manufacturing and then later in service. A particularly difficult problem in this regard is the reliable detection/monitoring of regions of weak bonding that may result from poor adhesion or poor cohesive strength, or degradation in service. One promising and perhaps less explored avenue we have recently begun to investigate for this purpose centers on the use of (chirped) fiber Bragg grating sensing technology. In this scenario, a grating is patterned into a fiber optic such that a (broadband) spectral reflectance is observed. The sensor is highly sensitive to local and uniform changes across the length of the grating. Initial efforts to evaluate this approach for measuring adhesive bonding defects at substrate interfaces are discussed.

Sandia National Laboratories is a multi-program laboratory managed and operated by Sandia Corporation, a wholly owned subsidiary of Lockheed Martin Corporation, for the U.S. Department of Energy's National Nuclear Security Administration under contract DE-AC04-94AL85000.

Keywords: Fiber Bragg grating, chirped, adhesion, epoxy, encapsulation, interface

1. INTRODUCTION

Encapsulated materials often fail in mechanical environments when there is poor adhesion at the component/encapsulant interface. For example, a thermoset polymer matrix which can easily delaminate from a metal component loses its effectiveness to insulate the component from stresses generated during vibrational modes or from localized electrical fields.[1-3] Fiber Bragg gratings (FBG) are often embedded into the bulk polymer matrix to measure stresses generated during encapsulation, cure shrinkage, extent of reaction, etc.[4-7] Application to adhesive interfaces has been carried out by placing FBGs into joint bond lines where a mechanical load is then applied until weak bonding/disbonds occur under shear.[8-12] Herein, we have set out to place the fiber at the surface of an encapsulant-component interface to monitor adhesion during encapsulation and any changes that arise due to physical aging. In this scenario, the FBG actually provides information about the surrounding stresses, which are quite complex, so for the sake of simplicity we are equating the stresses measured along the interface to adhesion in this work. Ultimately, it is our goal to use FBG data generated at the interface to build a finite elemental model which can be used to define adhesive integrity initially while in service as well as predict when failure will occur in the future.[3]

1.1 Background

The fiber Bragg grating sensor diagnostic is shown in Figure 1 and can be described as follows.[13-15] An optical fiber is exposed to UV light using a phase mask or via holographic techniques during fabrication. The light changes the local refractive index of the exposed glass regions thereby inducing a pattern. The pattern can be uniform (periodic) along the entire length of the exposed portion of the fiber or graduated (chirped) such that the spacing in the grating is smaller on one end and larger on the other. The length of the grating typically ranges from a couple millimeters to over one hundred.

When light from a superluminescent LED lightsource is directed into a chirped fiber, most of the light is transmitted except for a broadband spectral reflectance peak (that may be 1535-1560 nanometers) corresponding to the grating spacing. Any change in the grating spacing affects the reflected light which is referred to as the reflected Bragg signal.

For example, when the fiber grating is under tension, the reflected signal will shift to longer wavelengths. Likewise, when the fiber is under compression the signal will shift to shorter wavelengths. A non-uniform stress applied anywhere along the length of the chirped grating will affect the reflected signal at that location. Thus, it is possible to get local information about compression (or a lack thereof) at a particular point along the grating. The more common FBGs with a periodic spacing work similarly but since the grating spacing is uniform, local changes are not as discernable compared to chirped FBGs.

To determine the efficacy of both types of fibers for monitoring adhesion at component interfaces, fibers were mounted onto metallic or ceramic substrates and encapsulated using a well characterized epoxy system. Any regions of poor adhesion between the encapsulant and the substrate should be detected by the fiber Bragg grating sensor at t=0 and over the lifetime of the material.[13]

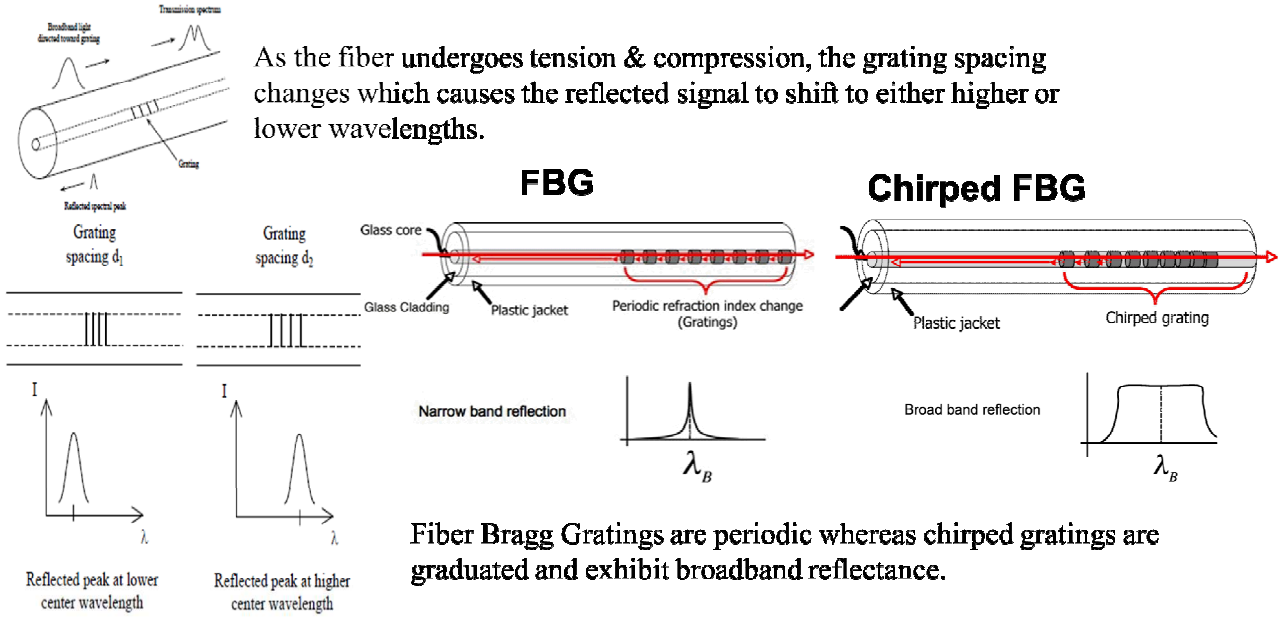

Figure 1. Fiber Bragg grating system; changes in the grating spacing translate into shifts in the reflected Bragg signal.

2. EXPERIMENTAL

2.1 FBG System

The fiber optic setup consisted of a Denselight DL-BP1-1501A Superluminescent LED Source (with Integrated Optical Circulator) and an I-MON 512E-USB 2.0 Interrogation Monitor. Fiber sensors consisted of the os1100 FBG from Micron Optics and four different custom-made chirped FBGs manufactured by Timbercon, Inc and O/E Land Inc. Each of the custom chirped FBGs were polyimide coated and had a central wavelength of ~1547-1548 nm. The only variance was in the reflectivity (> 80% vs 40-50%) and grating length (12, 80, or 100 mm).

2.2 Chemicals

Epon 828 resin was purchased from Miller-Stephenson, diethanolamine (DEA) curing agent was purchased from Acros Organics, and glass microballoons (D32) were purchased from 3M. All substrates were cleaned with Brulin 815GD. Fibers were attached to substrate interfaces using either EPO-TEK 353ND or Norland electronic Adhesive 121. In some instances, substrates were coated with Frekote 44-NC mold release purchased from Henkel or a made-to-order Epoxy Parfilm in Solvent A mold release from Price-Driscoll.

2.3 Fixturing

Two fixtures were machined and used to mount the sensor onto various substrate interfaces. The primary fixture consists of a micrometer, stage, and placement pins (Figure 2) such that a flat rectangular substrate is placed onto the

stage and the fiber is secured on one end using the UV or thermally cured epoxy. The opposite end of the fiber is then secured and pre-strained using a micrometer thereby placing the fiber sensor in intimate contact with the coupon surface.

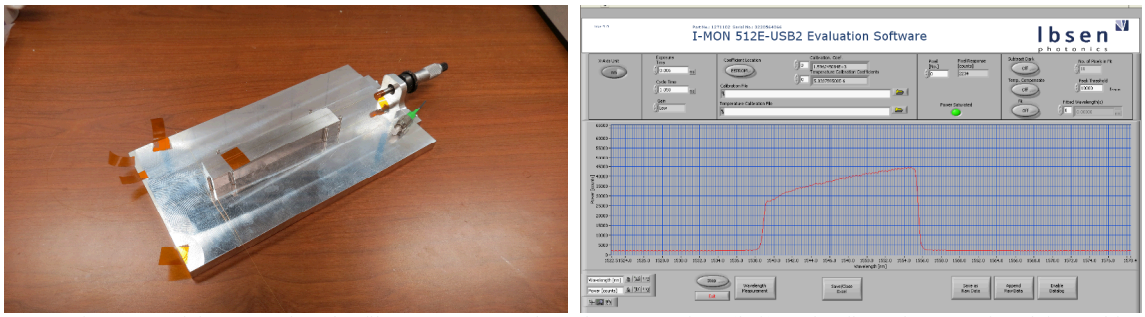

Figure 2. Fixture used for mounting the fiber sensor onto the substrate surface (left) and reflected Bragg signal for a chirped FBG secured to the interface (right).

We were also interested in mounting fibers to conical edges and cylinders so a secondary fixture designed after a bolo tie was machined from aluminum (Figure 3).

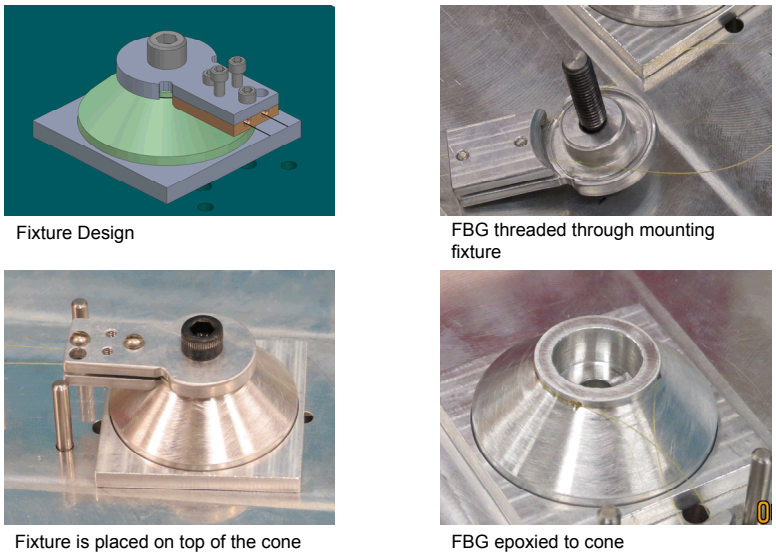

Figure 3. Fixture and process for mounting fibers to a high stress zone on a complex structure.

2.4 Processing

Epon 828 and DEA were pre-heated for 2 hours at 71 °C. The DEA was then added to the hot epoxy and stirred by hand for 5 minutes. The mixture was degassed at 71 °C for a sufficient amount of time and then poured onto the fiber/substrate. The epoxy was then cured in an oven isothermally for 24 hours at 71 °C or non-isothermally using a 2-tier profile with intermediate isothermal stage followed by thermal ramp to 71 °C. In either case the sample was allowed to cool slowly to room temperature when the profile was complete. In some instances, a filled encapsulant was used and prepared in an analogous manner but with pre-heated (71 °C) glass microballoons mixed into the Epon 828 and then DEA was added.

3. RESULTS AND DISCUSSION

We first set out to encapsulate a chirped fiber optic sensor onto a rectangular alumina substrate by affixing the fiber to the surface and pouring Epon 828/DEA onto the entire length of the grating (> 80%, 80 mm). The epoxy was then cured for 24 hours in an oven at 71 °C. Changes in the reflected Bragg signal were observed when the sample was cooled to room temperature compared to when the epoxy was initially poured onto the substrate. Results are shown in Figure 4 where the blue curve is t = 0 and the red curve is the encapsulated fiber sensor. The reflected Bragg signal shifted 0.129 nm on the short-wavelength end which equates to a fiber strain value of approximately 155 με. This relatively small

grating spacing change is due to the compression the fiber is experiencing from the encapsulant which is now bonded to the low surface energy substrate.[16-19] Shear stresses generated during curing and thermal stresses generated during cooling appear to be very low for this system.

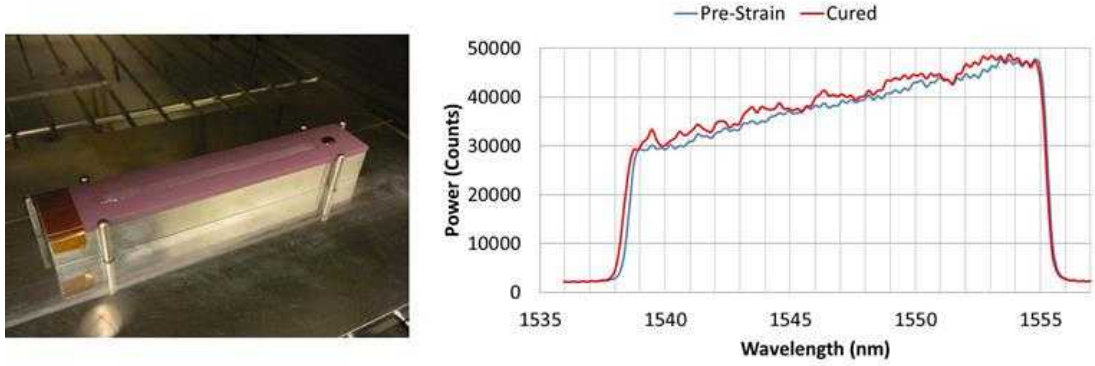

Figure 4. Chirped fiber Bragg grating sensor embedded on alumina substrate and reflected Bragg signals.

Our next experiment was aimed at demonstrating the ability of the fiber sensor to detect regions of poor adhesion. To accomplish this, we introduced artificial areas of poor adhesion at several locations along the length of the substrate. A chirped fiber (> 80%, 80 mm) was mounted onto the surface and PTFE tape was placed over the fiber in two locations. Subsequently, Epon 828/DEA was poured along the entire length of the grating and curing was carried out in the oven (71 °C, 24h). Results for both alumina and aluminum are shown in Figure 5. Similar behavior of the reflected Bragg signal was observed in both cases – local regions along the grating where there was poor adhesion due to the PTFE were easily distinguishable from areas where there was good adhesion.

In the case of the alumina sample, the short-wavelength end of the fiber shifted about 0.066 nm (80 με) which is on the same order of magnitude observed in the first experiment. Two distinct wells were evident in the reflected signal which corresponds to the location of the PTFE tape. The magnitude of the well on the long-wavelength end of the fiber was less than for the shorter wavelength end and the intensity of the signal across the long-wavelength end was quite different after curing. This can be explained by the non-uniformity of the encapsulant delivered along the length of the grating and post mortem analysis which revealed some epoxy had wicked under the PTFE in that location.

Two wells were also observed for the fiber encapsulated onto the aluminum substrate but in this instance the Bragg shift was a much larger one at 0.802 nm (963 με). This substrate dependent behavior of the fiber is most likely a result of the aluminum having a much higher surface energy (roughness) as opposed to the argument of CTE mismatch. The CTE of aluminum is about 4 times greater than that of alumina so it is in better agreement with the high CTE polymer. Finally, the intensity difference before and after curing is probably a result of encapsulant non-uniformity as well as the output of the light source which is more difficult to normalize than for newer fiber optic interrogation systems. Nonetheless, as evident in the wells of the reflected signals, the sensitivity of the fiber to the regions of poor adhesion is remarkable and clearly demonstrates that they can be used for the purpose of monitoring adhesion at an interface.

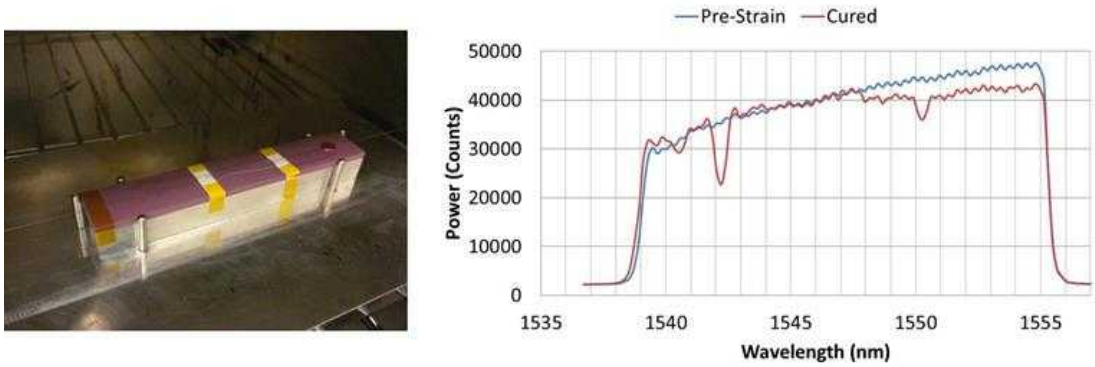

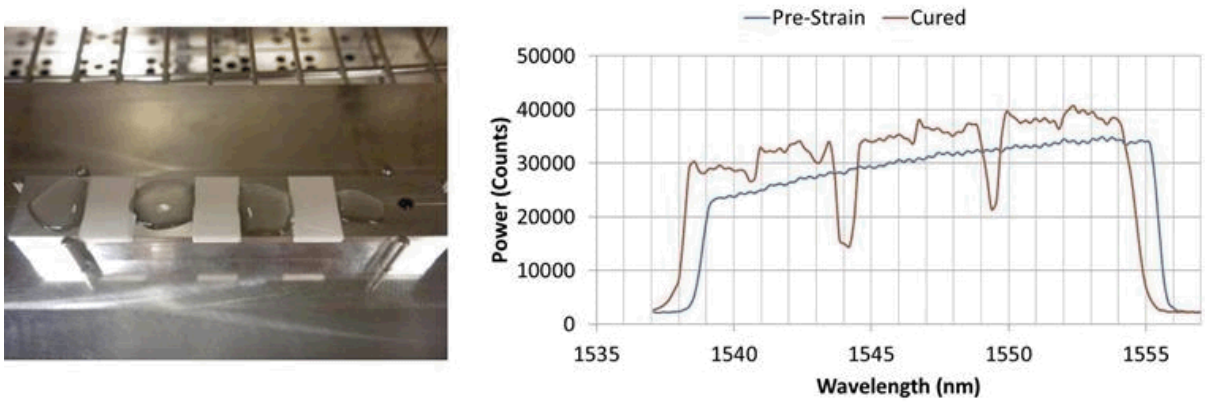

Figure 5. Embedded fiber sensor with induced areas of poor adhesion on alumina (top) and aluminum (bottom). The reflected Bragg signals are shown on the right.

Our next objective was to investigate sensitivity for contamination at the substrate interface. Fiber Bragg sensors (os1100) were mounted onto the surface of flat aluminum coupons coated with or without mold release contamination. Epon 828/DEA was then poured onto the FBG and the sample was cured in the oven (71 °C, 24h). Adhesion influences due to epoxy Parfilm mold release (Ultra II) was evaluated by comparing the reflected Bragg signals (Figure 6) and from delamination experiments. The encapsulated fiber on the mold released substrate experienced a Bragg shift of 0.192 nm (230 με) whereas the non-mold released substrate led to a shift of 0.974 nm (1169 με). Thus, the shift in the reflected Bragg signal after curing was much greater for the clean versus contaminated substrate. There was no evidence of wicking and the epoxy easily delaminated from the interface for the mold released substrate. These results suggest that the fiber is sensitive to poor adhesion along the length of the grating brought on by mold release contamination.

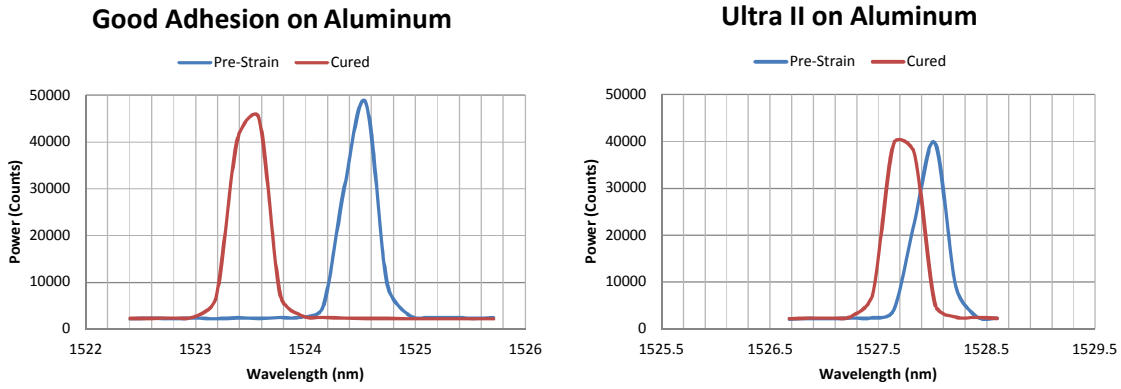

Figure 6. Reflected Bragg signals for encapsulated fibers on clean (left) and mold release contaminated substrates (right).

A lower reflectivity chirped FBG (40-50%, 100 mm) was sensitive to non-uniform contamination from mold release as well. The sensor was mounted onto the surface of a flat aluminum coupon contaminated with FreeKote mold release (2 spots). Epon 828/DEA was then poured onto the chirped FBG sensor and the epoxy was cured in an oven (71 °C, 24 h). Poor adhesion due to the mold release contamination at the two spots led to local changes in the reflected Bragg signal (Figure 7). The mold release serves as a strain release at the two spots. Thus, the lower reflectivity chirped FBG is sensitive to local changes in adhesion along the length of the grating.

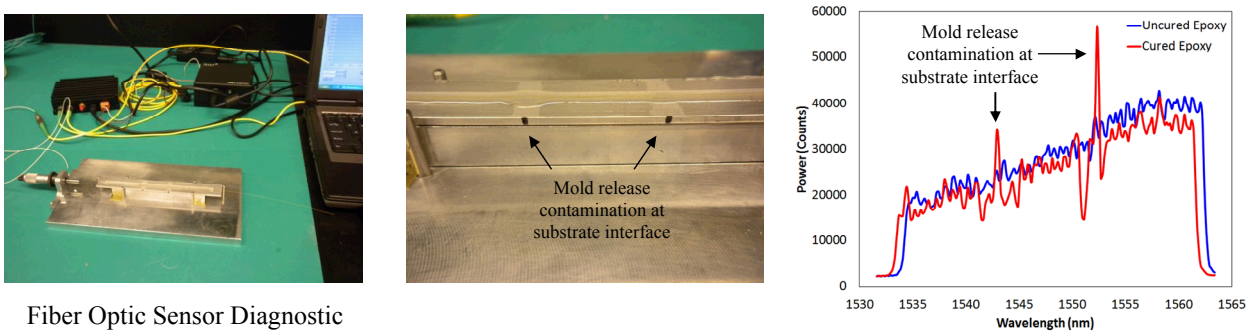

Figure 7. Fiber Bragg grating system (left); mold release contamination on aluminum substrate (middle); and reflected Bragg signals (right) demonstrating the fibers ability to measure poor adhesion locally.

Parallel to the work with the aluminum substrates was an experiment to induce a dis-bond in a sample of encapsulated fiber sensor on a flat alumina substrate. A video (Video/Audio 1) was made for this experiment where the dis-bond was introduced by cracking the epoxy around one end of the embedded fiber. When the crack occurred, the local reflected Bragg signal corresponding to that location on the grating changed due to decreased compression from the broken epoxy. However, the fiber did not break which suggests that the sensors have some propensity for withstanding severe changes in the local environment such as in adhesive failure without creating structural failure of the fiber.

Video/Audio 1. Cracking epoxy on one end of an encapsulated fiber. http://dx.doi.org/doi.number.goes.here

We next shifted our attention to optimizing the ability of the fiber to more precisely monitor interfacial adhesion. Delamination experiments had shown that the epoxy could potentially wick between the fiber and the substrate (Figure 5, top right) so we identified specific handling/processing techniques to ensure that the sensor was providing more information about the interface relative to the bulk epoxy. To demonstrate the effectiveness of these techniques, we performed an experiment to show behavior of fiber embedded in the bulk. This was accomplished by placing ½ of chirped FBG (> 80%, 80 mm) into the bulk epoxy and leaving the remaining ½ in air in an experiment similar to that carried out by Cusano et al.[20] Overall, the Bragg signal for the embedded fiber shifted 4.925 nm (5911 $\mu\varepsilon$) whereas the free portion of the fiber experienced no change (Figure 8) which was consistent with Cusano et al.

The strain the chirped FBG sensor experienced in the bulk epoxy was significantly larger than what was observed at the interface. Again, the fiber experiences compression from the encapsulant which is bonded to the substrate in that case. These results suggested that it was probably better to use a larger free volume of encapsulant in adhesion experiments going forward.

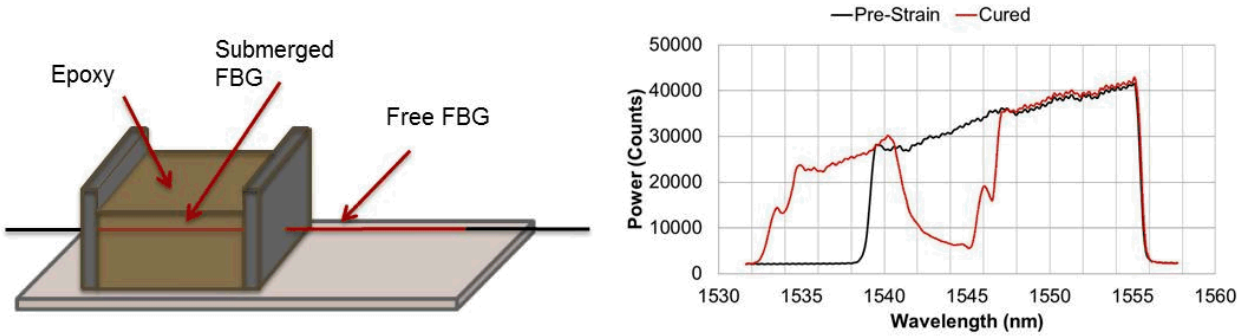

Figure 8. Fiber sensor embedded in the bulk epoxy and reflected Bragg signals.

Encapsulated components are not always rectangular and flat so we next turned our attention to more complex geometries. These consisted of conical edges and cylinders machined from alumina or aluminum metal. In a relatively facile experiment, an FBG (os1100) was mounted onto a high stress edge of a conical geometry and encapsulated using Epon 828/DEA (71 °C, 24h). The results are shown in Figure 9 where the reflected Bragg wavelength shifted 1.745 nm which equates to 2094 $\mu\varepsilon$. Though the bend radius for the fiber is small (>17 mm) and most fragile along the grating, this illustration shows that it can still be mounted to interfaces with complex geometries and used to monitor adhesion at that interface.

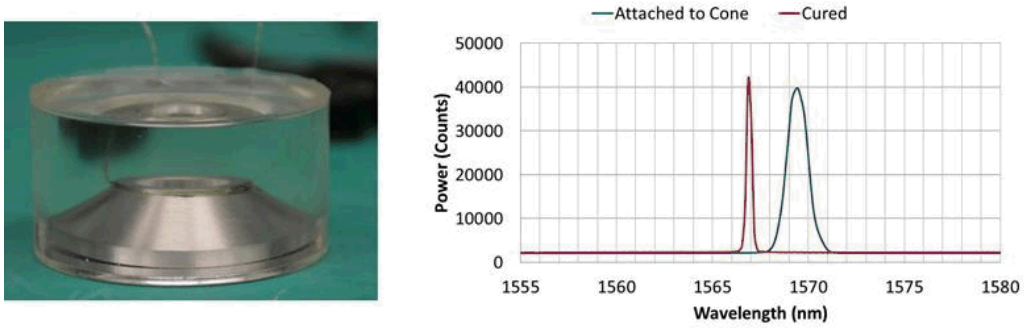

Figure 9. Fiber sensor mounted onto a conical shaped aluminum sample that was encapsulated using Epon 828/DEA and reflected Bragg signals.

A chirped FBG (40-50%, 12 mm) was also successfully mounted at the same location. The substrate was then placed into a plastic cup and encapsulated with Epon 828/DEA (24h, 71 °C). As shown in Figure 10, the reflected Bragg signal shifted approximately 2 nm which corresponds to the fiber experiencing 2400 με due to compression between the epoxy and the aluminum substrate. No discernable difference was observed along the length of the grating suggesting uniform adhesion.

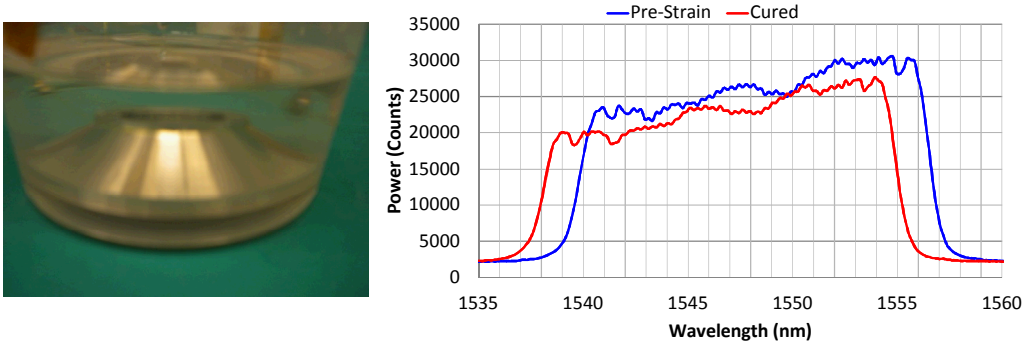

Figure 10. Chirped FBGs were attached to complex geometries and used to monitor adhesion.

We next turned to a filled system to see what effect that would have on the Bragg signal. This was achieved by mounting a chirped FBG (40-50%, 12 mm) onto the same curved edge of another aluminum substrate followed by encapsulation with Epon 828/GMB/DEA (24 h, 71 °C). As shown in Figure 11, the reflected Bragg signal shifted approximately 1 nm (1200 με) which appears to be under uniform compression (adhesion). Though it is ill-advised to draw multiple conclusions from a single data point, it is clear that the reflected Bragg signal for the unfilled was roughly twice that of the filled in this experiment. The nature of this difference is beyond the scope of this work at this time but will be discussed at a later point. Ultimately, these experiments demonstrate that the fiber is able to monitor adhesion in both filled and unfilled encapsulants and that adhesion with this particular filled encapsulant appears to be uniform along the entire length (13 mm) of the grating.

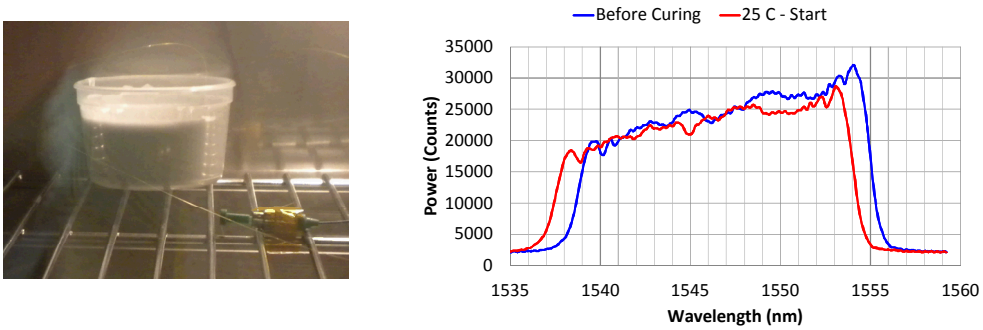

Figure 11. A chirped FBG was mounted to a curved aluminum edge and used to measure adhesion with a filled encapsulant.

Further confirmation that FBGs could be mounted to a myriad of complex geometries and used to measure adhesion was also achieved. An FBG (os1100) was affixed to an aluminum cylinder whose diameter was identical to the curved edge conical geometry and encapsulated in an analagous manner. A shift of about 1.2 nm (1200 με) was observed for the unfilled encapsulant (Figure 12).

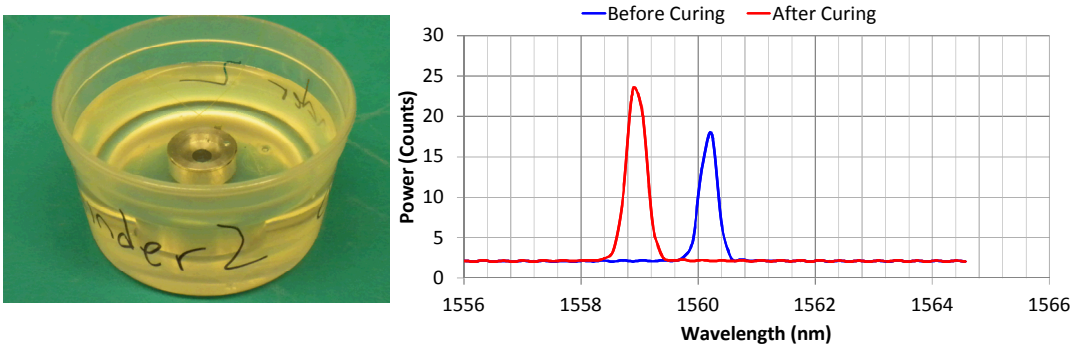

Figure 12. FBGs mounted to an aluminum cyclinder and encapsulated with unfilled epoxy.

Our next objective was to gauge an embedded fiber's ability to measure delamination or changes during thermal cycling. This was accomplished using Department of Defense Test Method Standard Mil-Std-810G Section 520. The unfilled sample shown in Figure 10 was subjected to this thermal cycle profile. During the first cycle (on cold), the reflected Bragg signal shifted to shorter wavelengths due to the fiber experiencing more compression at the interface. The compression continued to increase until a crack occurred in the epoxy around the 50 minute point of the first cycle which was sufficient enough to break the epoxy around the fiber as observed by the local Bragg shift change (Figure 13). The crack presumably occurred due to high shear stresses from CTE mismatch between the unfilled epoxy and the aluminum substrate.

We note that we were able to determine the location of the crack as well as monitor compression at the interface during thermal cycling using the chirped FBG for the 3 cycles that were carried out (more are possible). The remaining portion of the intact fiber appeared to experience the same amount of compression before and after thermal cycling. This experiment was carried out in duplicate with the filled encapsulant sample shown in Figure 11 but in this case a crack

did not occur and the Bragg shift was identical before and after thermal cycling. These results highlight the utility of this approach for real-time and in situ monitoring of adhesive integrity in a variety of thermal environments.

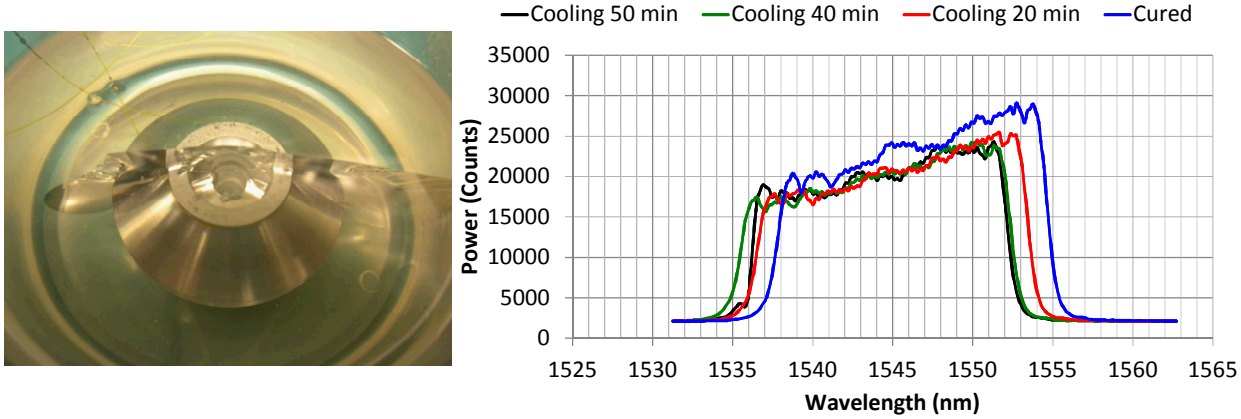

Figure 13. Chirped FBG mounted to an aluminum substrate detects a crack in the encapsulant during thermal cycling.

Up to this point, experiments were carried out on complex substrates machined from aluminum and isothermally cured. Though we were able to demonstrate feasibility and define processing using this approach, our hypothesis was that this preparative work would seamlessly translate to the more expensive alumina substrate which could then be encapsulated using an alternate cure schedule. To prove this notion, a chirped fiber (40-50%, 12 mm) was successfully mounted to a curved edge of alumina substrate and encapsulated using Epon 828/DEA (Figure 14) using the non-isothermal cure profile outlined in the experimental section. The embedded fiber sensor experienced uniform compression along the length of the grating and the overall reflected Bragg signal shifted approx. 1 nm which equates to 1200 με.

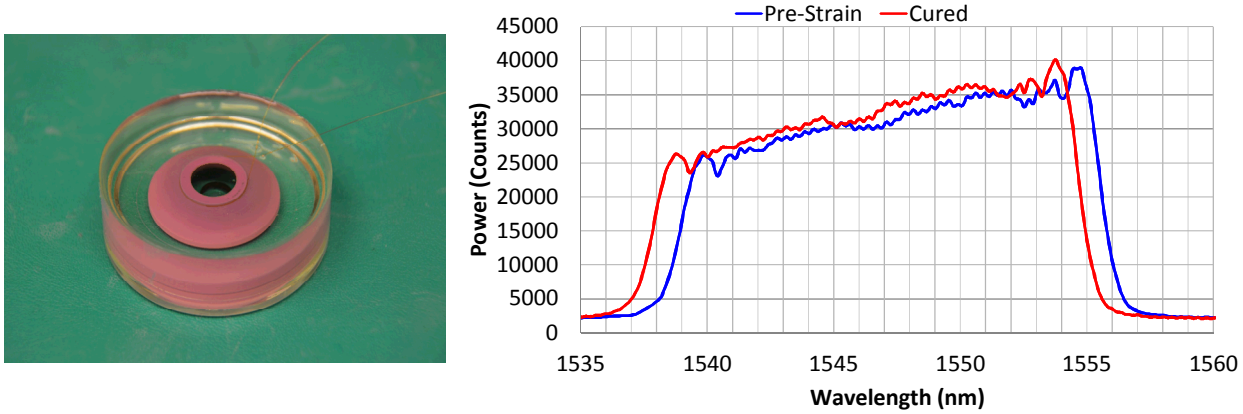

Figure 14. A chirped FBG is mounted to an alumina substrate and used to measure adhesion.

Our last effort was focused on a physical aging study which occurred over the course of 1 ½ years so as to evaluate shelf-life influence on adhesion. The embedded FBG shown in Figure 9 was left on the shelf and its adhesion monitored after 3, and 13 months (Figure 15). Overall, the fiber appears to be experiencing a slight decrease in compression at the interface as the sample ages, which is perhaps due to shear stress relaxation over time. It seems unlikely that the fiber is slipping over time since it is well understood that there is excellent strain transfer efficiency between the polyimide coating and the surrounding epoxy matrix and the strain value is within the operating window of the sensor (5000 με). It also not likely that the FBG itself is changing over time as their long lifetimes are well established.[13] Accelerated and physical aging studies currently being carried out in our lab should reveal more about this interesting phenomena which will ultimately help us reach the goal of using FBG data generated at the interface to build a finite elemental model which can be used to define adhesive integrity initially while in service as well as predict when failure will occur in the

future. For the time being, it is clear that there are changes in adhesion due to aging which fiber optic sensors are able to detect.

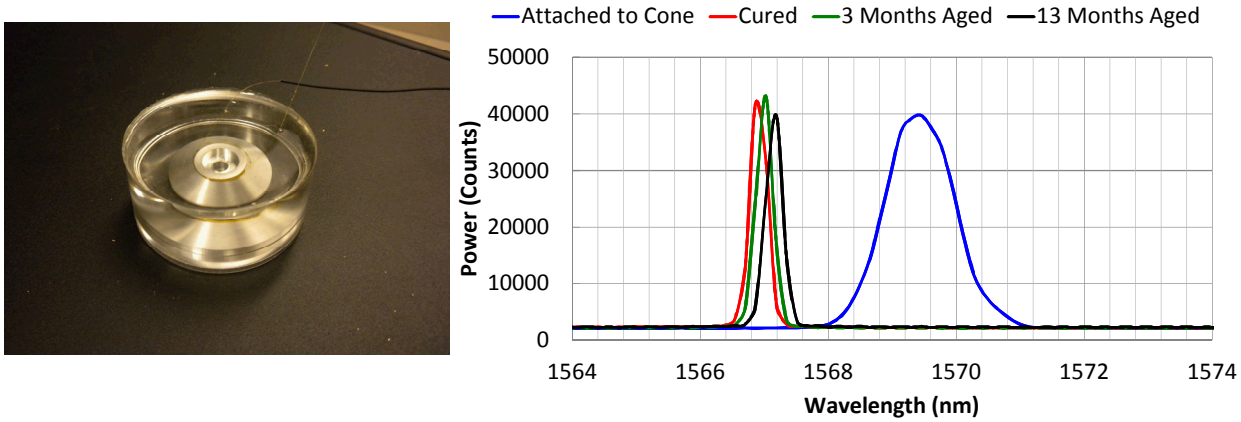

Figure 15. FBG mounted to an aluminum substrate aged over the course of 18 months.

4. CONCLUSIONS

This relatively new technology has shown great promise in the area of weak bond detection at interfaces of encapsulated components. The chirped fiber Bragg grating sensors are relatively inexpensive and offer real time data acquisition, spatial sensitivity, mobility, and substrate adaptability. The resolution is superior to other non-destructive evaluation methods such as X-Ray and ultrasonics which do not work well for filled systems. In this report, fibers were mounted to both flat and complex geometries that were clean and/or contaminated with mold release. The systems were then encapsulated with Epon 828/DEA or 828/DEA/GMB and used to successfully measure adhesion post curing, during thermal cycling, and physical aging. In the future, we plan to use them to measure the effects of adhesion promoters (silane coupling agents) at the substrate interface, measure bulk encapsulant stresses brought on by nonisothermal cure profiles, and investigate boundary stresses for binary interfaces.

REFERENCES

[1] Chambers, R. S.; Lagasse, R. R.; Guess, T. R.; Plazek, D. J.; Bero, C. *Journal of Electronic Packaging* **1995**, *117*, 249.
[2] Adolf, D. B.; Stavig, M. E.; Kawaguchi, S.; Chambers, R. S. *J. Adhes.* **2007**, *83*, 85.
[3] Adolf, D. B.; Chambers, R. S.; Hance, B.; Elisberg, B. *J. Adhes.* **2010**, *86*, 1111.
[4] Giordano, M.; Laudati, A.; Nasser, J.; Nicolais, L.; Cusano, A.; Cutolo, A. *Sens. Actuator A-Phys.* **2004**, *113*, 166.
[5] Harsch, M.; Karger-Kocsis, J.; Herzog, F. *Macromolecular Materials and Engineering* **2007**, *292*, 474.
[6] Wang, Y.; Han, B.; Kim, D. W.; Bar-Cohen, A.; Joseph, P. *Exp. Mech.* **2008**, *48*, 107.
[7] Case, S. L.; O'Brien, E. P.; Ward, T. C. *Polymer* **2005**, *46*, 10831.
[8] Capell, T. F.; Palaniappan, J.; Ogin, S. L.; Thorne, A. M.; Reed, G. T.; Crocombe, A. D.; Tjin, S. C.; Wang, Y.; Guo, Y. *Plastics Rubber and Composites* **2009**, *38*, 138.
[9] Li, H. C. H.; Herszberg, I.; Mouritz, A. P.; Davis, C. E.; Galea, S. C. *Compos. Struct.* **2004**, *66*, 239.
[10] Trego, A.; Keller, R., *Fiber optics in bonded repairs*. Soc Advancement Material & Process Engineering: Covina, 2002; p 1647-1661.
[11] Murayama, H.; Kageyama, K.; Naruse, H.; Shimada, A.; Uzawa, K. *J. Intell. Mater. Syst. Struct.* **2003**, *14*, 3.
[12] Schulz, W. L.; Udd, E.; Morrell, M.; Seim, J.; Perez, I.; Trego, A. In *Nondestructive Evaluation of Aging Aircraft, Airports, and Aerospace Hardware Iii*; Mal, A. K., Ed.; Spie-Int Soc Optical Engineering: Bellingham, 1999; Vol. 3586, p 41.
[13] Kashyap, R. *Fiber Bragg Gratings (Second Edition)*; Academic Press, 2010.
[14] Measures, R. M. *Structural Monitoring with Fiber Optic Technology*; Academic Press, 2001.
[15] Udd, E. *Proc. IEEE* **1996**, *84*, 60.

[16] Yang, S.; Gu, L.; Gibson, R. F. *Compos. Struct.* **2001**, *51*, 63.
[17] Nagy, P. B. *Journal of Nondestructive Evaluation* **1992**, *11*, 127.
[18] Kumar, R. L. V.; Bhat, M. R.; Murthy, C. R. L. *Int. J. Adhes. Adhes.* **2013**, *42*, 60.
[19] Vine, K.; Cawley, P.; Kinloch, A. J. *J. Adhes.* **2001**, *77*, 125.
[20] Cusano, A.; Capoluongo, P.; Cutolo, A.; Giordano, M. *IEEE Sens. J.* **2006**, *6*, 111.